Plant Direct

WILEY

American Society of Plant Biologists SEB SOCIETY FOR EXPERIMENTAL BIOLOGY

RESEARCH ARTICLE OPEN ACCESS

Suppression of Chorismate Mutase 1 in Hybrid Poplar to Investigate Potential Redundancy in the Supply of Lignin Precursors

Yaseen Mottiar[1,2] | Timothy J. Tschaplinski[3] | John Ralph[4,5] | Shawn D. Mansfield[1,6,5]

[1]Department of Wood Science, University of British Columbia, Vancouver, British Columbia, Canada | [2]Department of Biology, University of Ottawa, Ottawa, Ontario, Canada | [3]Center for Bioenergy Innovation, Oak Ridge National Laboratory, Oak Ridge, Tennessee, USA | [4]Department of Biochemistry, University of Wisconsin, Madison, Wisconsin, USA | [5]Department of Energy Great Lakes Bioenergy Research Center, Wisconsin Energy Institute, Madison, Wisconsin, USA | [6]Department of Botany, University of British Columbia, Vancouver, British Columbia, Canada

Correspondence: Yaseen Mottiar (ymottiar@uottawa.ca) | Shawn D. Mansfield (shawn.mansfield@ubc.ca)

Received: 15 August 2024 | **Revised:** 3 February 2025 | **Accepted:** 6 February 2025

Funding: Financial support for this work was provided by a Korea Institute of Science and Technology grant to S.D.M. by the Great Lakes Bioenergy Research Center, U.S. Department of Energy, Office of Science, Office of Biological and Environmental Research, under Award Number DE-SC0018409 to S.D.M. and J.R., and by the Center for Bioenergy Innovation, U.S. Department of Energy, Office of Science, Office of Biological and Environmental Research, under Award Number FWP ERKP886 to T.J.T. This manuscript has been supported by UT-Battelle LLC, under Contract No. DE-AC05-00OR22725 with the U.S. Department of Energy.

Keywords: aromatic amino acids | lignin biosynthesis | RNAi | salicylic acid | shikimate pathway

ABSTRACT

Chorismate is an important branchpoint metabolite in the biosynthesis of lignin and a wide array of metabolites in plants. Chorismate mutase (CM), the enzyme responsible for transforming chorismate into prephenate, is a key regulator of metabolic flux towards the synthesis of aromatic amino acids and onwards to lignin. We examined three CM genes in hybrid poplar (*Populus alba*×*grandidentata; P39*, abbreviated as *Pa*×*g*) and used RNA interference (RNAi) to suppress the expression of *Pa*×*g*CM1, the most highly expressed isoform found in xylem tissue. Although this strategy was successful in disrupting *Pa*×*g*CM1 transcripts, there was also an unanticipated increase in lignin content, a shift towards guaiacyl lignin units, and more xylem vessels with smaller lumen areas, at least in the most severely affected transgenic line. This was accompanied by compensatory expression of the other two CM isoforms, *Pa*×*g*CM2 and *Pa*×*g*CM3, as well as widespread changes in gene expression and metabolism. This study investigates potential redundancy within the CM gene family in the developing xylem of poplar and highlights the pivotal role of chorismate in plant metabolism, development, and physiology.

1 | Introduction

Lignin is a phenolic polymer found in vascular plants wherein it provides structural support and contributes to water conduction and defense. The deposition of lignin rigidifies secondary cell walls and helps adjoining cells adhere by reinforcing the middle lamella (Gibson 2012; Mottiar et al. 2020). Lignified cell walls in the plant vasculature have reduced permeability, which enables long-distance water transport (Sperry 2003). Similarly, the stability and insolubility of lignin provide a physical and chemical barrier that helps guard against pests and pathogens (Miedes et al. 2014). However, the recalcitrance of lignin to biological and chemical degradation hinders the efficient industrial processing of plant biomass (Li, Pu, and Ragauskas 2016). As such, there is tremendous value in studying lignin biosynthesis.

Lignin is assembled primarily from three hydroxycinnamate derivatives known as monolignols — *p*-coumaryl, coniferyl,

and sinapyl alcohol — that give rise to *p*-hydroxyphenyl (H), guaiacyl (G), and syringyl (S) units in lignin polymers (Boerjan, Ralph, and Baucher 2003). The monolignols are produced via the phenylpropanoid pathway from phenylalanine and, in grasses, from tyrosine as well (Cass et al. 2015; Mottiar et al. 2016). As lignin typically comprises 20%–35% of the dry weight of plants, vast amounts of photosynthetic carbon are allocated to the phenylpropanoid pathway. Lignin formation is energetically costly, and it has been estimated that 0.975–1.724 moles of translocated sucrose are needed to produce every mole of monolignol, depending upon which specific biosynthetic route is followed (Amthor 2003). Accordingly, lignin biosynthesis is tightly regulated at the levels of transcription, posttranslational modification, allostery, and the supply of substrates for polymerization (Zhong and Ye 2009; Wang et al. 2019; Behr et al. 2019).

The shikimate and aromatic amino acid pathways, which lie upstream of phenylpropanoid biosynthesis, are responsible for the production of phenylalanine and tyrosine (Maeda and Dudareva 2012). Through a series of enzymatic conversions, the shikimate pathway transforms phosphoenolpyruvate and erythrose 4-phosphate, both products of carbohydrate metabolism via glycolysis and the pentose phosphate pathway, into chorismate (Bonner and Jensen 1998). In addition to the phenylpropanoids, chorismate is also a precursor to folates, indoles, phylloquinone, anthranilate, and salicylic acid, as well as proteins via phenylalanine, tyrosine, and tryptophan (Herrmann 1995; Mustafa and Verpoorte 2005; Bowsher, Steer, and Tobin 2008; Tzin and Galili 2010; Tohge et al. 2013). Consequently, chorismate represents an important branchpoint at the junction of a plethora of metabolites in plants (Figure 1).

Chorismate mutase (CM) catalyzes the pericyclic Claisen rearrangement of chorismate to form prephenate, a precursor to both phenylalanine and tyrosine (Gorisch 1978; Romero, Roberts, and Phillipson 1995). Previous reports suggest that vascular plants typically have two or three CM isozymes with one of these occurring in the cytosol (Woodin, Nishioka, and Hsu 1978; d'Amato et al. 1984; Poulsen and Verpoorte 1991). In Arabidopsis, for example, CM1 and CM3 contain plastid-localization signals and are allosterically regulated by aromatic amino acids, whereas CM2 is cytosolic and allosterically insensitive (Eberhard et al. 1996; Mobley, Kunkel, and Keith 1999). A complete cytosolic pathway for the biosynthesis of aromatic amino acids from chorismate has been uncovered in recent years (Qian et al. 2019), further illustrating the metabolic divarications that occur at chorismate.

The specific contributions of the various CM isoforms to lignin biosynthesis have not been extensively characterized. However, CM1 is the most strongly expressed of the three CM genes in the stems of Arabidopsis (Ehlting et al. 2005) and poplar (Tsai et al. 2006), in which there exist vast metabolic requirements for phenylalanine to supply lignin precursors. Conversely, CM2 and CM3 are not constitutively highly expressed during xylem differentiation. Herein, we used RNA interference (RNAi) to suppress the expression of CM1 in hybrid poplar (*Populus alba*×*grandidentata*; P39, abbreviated as *Pa*×*g*) in order to investigate the role of CM in lignification. We found evidence of a potential redundancy in the CM gene family, but further studies will be needed to validate this finding.

2 | Materials and Methods

2.1 | Phylogenetic Analysis

The three CM sequences from Arabidopsis (*At*CM1, AT3G29200, Eberhard et al. 1993; *At*CM2, AT5G10870, Eberhard et al. 1996; and *At*CM3, AT1G69370, Mobley, Kunkel, and Keith 1999) were used as queries in BLAST searches to identify CM homologues from the reference genomes of *Populus trichocarpa* (JGI v4.1), *Amborella trichopoda* (AGP v1.0), *Brachypodium distachyon* (JGI v3.2), *Brassica rapa* (JGI FPsc v1.3), *Eucalyptus grandis* (JGI v2.0), *Medicago truncatula* (MTGD Mt4.0), *Oryza sativa* (RGAP v7.0), *Phaseolus vulgaris* (JGI v2.1), *Physcomitrium patens* (JGI v3.3), *Picea abies* (SGP v1.0), *Selaginella moellendorffii* (JGI v1.0), *Solanum tuberosum* (PGSC v4.03), *Vitis vinifera* (Genoscope 12X v2.1), and *Zea mays* (MGSP B73 RefGen_v4). These amino acid sequences were aligned using MEGA X with the MUSCLE algorithm and the default parameters (Kumar et al. 2018) and then used in the assembly of a maximum likelihood phylogenetic tree. CM sequences from the yeast *Saccharomyces cerevisiae* (*Sc*CM, YPR060C, Ball et al. 1986), the red alga *Porphyra umbilicalis* (Pum2195s0001.1.p, JGI v1.5), and the green alga *Chlamydomonas reinhardtii* (Cre03.g155200.t1.1, JGI v5.6) were used as an outgroup, and the tree was resampled using 1000 bootstrap iterations. Pairwise alignments of the poplar and Arabidopsis homologues were then inspected more closely (Figure S1A). Sequence identity and similarity values were calculated using the SMS Ident and Sim tool (Stothard 2000), and signal peptide predictions were conducted using TargetP-2.0 (Armenteros et al. 2019).

2.2 | RNAi-Mediated Suppression of CM1 in Poplar

The CM1 coding sequence was cloned from hybrid poplar (*Populus alba*×*grandidentata*; P39). RNA was isolated using a CTAB-based protocol (Kolosova et al. 2004) from the leaves of poplar plants that were flash-frozen in liquid nitrogen and ground into a powder with a mortar and pestle. This total RNA preparation was treated with DNase using the Turbo DNA-free kit (Life Technologies, Carlsbad, CA, USA) and then used in the synthesis of first-stand cDNA using the iScript cDNA synthesis kit (Bio-Rad Laboratories Inc., Hercules, CA, USA). Primers designed to anneal within the upstream and downstream regions were initially used for gene amplification and were designed based on the *Populus trichocarpa* reference genome (see Table S1 for all primer sequences and reaction conditions). After sequencing this amplicon to identify any polymorphisms (Figure S1B), a 400-bp fragment was amplified with *attB* adaptor sequences to enable Gateway cloning, and was then transferred into the pDON221 vector using BP Clonase (Life Technologies). Finally, an RNAi expression cassette was assembled by transferring this fragment from pDONR221 into pHELLSGATE12 (Helliwell and Waterhouse 2003) using LR Clonase (Life Technologies).

Chemically competent *Agrobacterium tumefaciens* EHA105 was transformed with the pHELLSGATE12 expression cassette following a freeze–thaw protocol (Wise, Liu, and Binns 2006). Next, leaf discs harvested from hybrid poplar plants grown in tissue culture were used for *Agrobacterium*-mediated transformation, as described previously (Mottiar

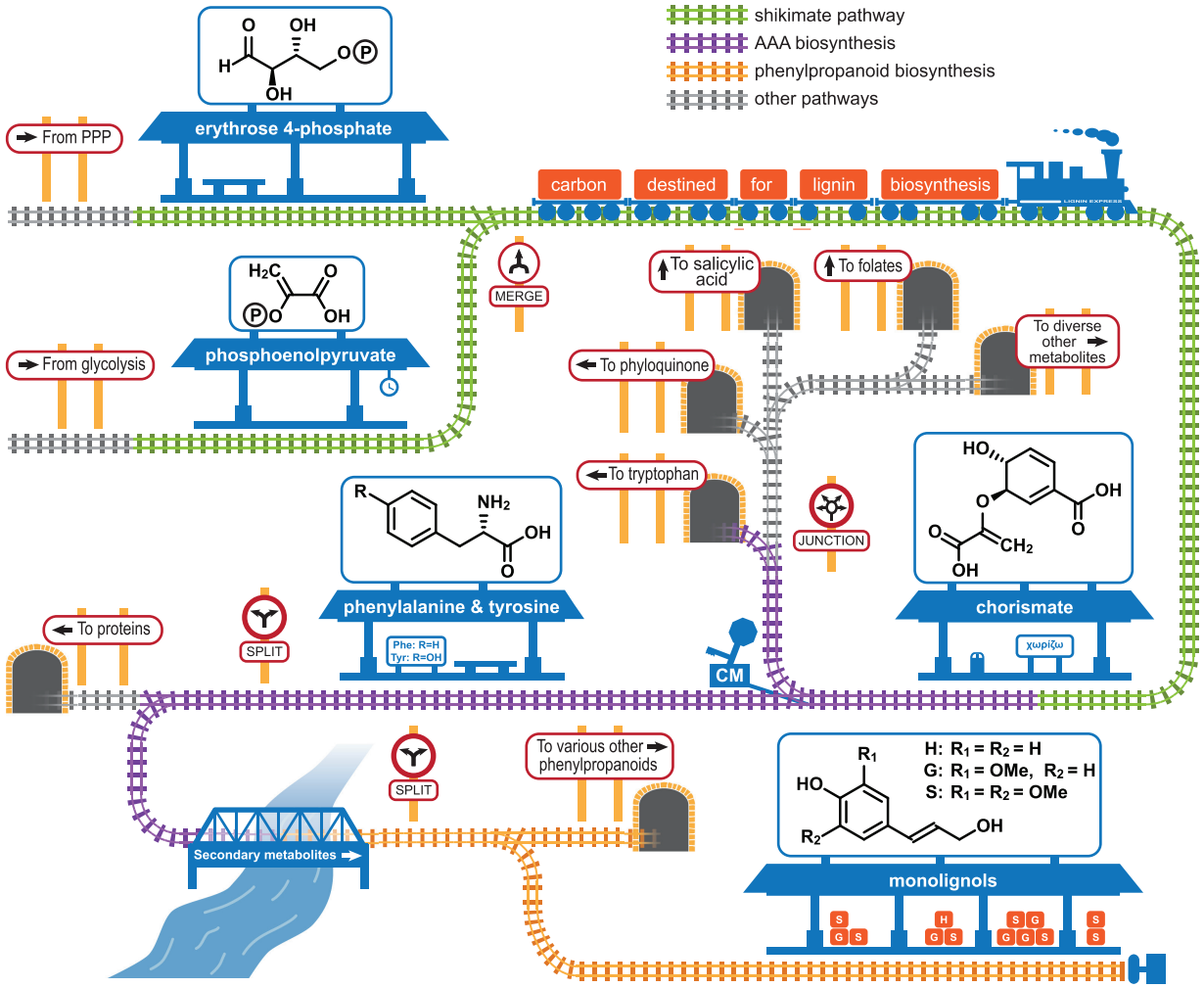

FIGURE 1 | Chorismate is a key branchpoint metabolite in plants. A biosynthetic map depicting the shikimate, aromatic amino acid (AAA), and phenylpropanoid biosynthetic pathways. Erythrose 4-phosphate from the pentose phosphate pathway (PPP) and phosphoenolpyruvate from glycolysis are combined and converted via the shikimate pathway (green) to produce chorismate. Next, chorismate is converted into phenylalanine, tyrosine, or tryptophan via the aromatic amino acid pathway (purple), or it can follow a series of alternate metabolic routes to produce various other metabolites. Phenylalanine and, in grasses, tyrosine can be further transformed via the phenylpropanoid pathway (orange) to produce various phenylpropanoid metabolites, including the monolignols that are used to produce lignin. As depicted, CM is an important metabolic gatekeeper enzyme upstream of lignin and phenylpropanoid biosynthesis.

et al. 2023). Positive transformants were selected on media containing hygromycin and were confirmed using semi-quantitative RT-PCR. Three PCR-positive lines were further propagated in tissue culture. All biological replicates were ultimately derived from apical stem pieces after several rounds of propagation.

Well-rooted plants were transferred into potting soil and grown in a greenhouse where natural lighting was supplemented with high-pressure sodium lamps (to a minimum of 500 μmol m^{-2} s^{-1}). The trees were supported with bamboo stakes, watered daily with fertigated water, and monitored for any signs of pests or disease. After 20 weeks, the bamboo stakes were removed, the trees were harvested, and the leaves and bark were carefully removed. Young leaves were collected and developing xylem tissue was scraped from the debarked stems, and then both were flash-frozen in liquid nitrogen and ground into a powder with a mortar and pestle. The debarked stems were air-dried and subsequently comminuted into a powder using a Wiley mill fitted with a 40-mesh sieve.

2.3 | Gene Expression

RNA was isolated from the frozen powder of young leaves and developing xylem as described above. Also as above, the RNA was then treated with DNase and converted into first-strand cDNA. These cDNA preparations were diluted eight-fold and subjected to RT-qPCR analysis with gene-specific primers that had been tested over a wide range of template concentrations and found to have good priming efficiency. Thermal cycling, fluorescence detection, and melt curve analysis were performed using a CFX 96 Real-Time PCR instrument with the corresponding CFX Manager software (Bio-Rad Laboratories). Primers specific to the poplar elongation factor 1β gene were used as a reference for the calculation of relative expression.

Prior to RNA-seq analysis, RNA preparations from developing xylem were assessed for yield and quality using an Agilent 2100 Bioanalyzer (Agilent Technologies) to ensure that all samples had RNA integrity numbers exceeding 9. Next, sequencing libraries were prepared using the TruSeq Stranded mRNA kit (Illumina Inc., San Diego, CA, USA) with 500 ng of purified RNA, and high-throughput sequencing was performed using a NextSeq 500 sequencer (Illumina Inc.). Sequence reads were then aligned to the *Populus trichocarpa* reference genome and analyzed as described elsewhere (Huang et al. 2024). Differentially expressed genes were evaluated based on triplicate samples of Line 3 and wild-type (WT) xylem RNA and were expressed as $\log_2$(fold change in expression). Finally, a gene ontology (GO) term enrichment analysis was performed with the PopGenIE tool using a false discovery rate correction for *p*-values (Sundell et al. 2015) with genes that were significantly upregulated (i.e., $\log_2$[fold change in expression] > 2) or significantly downregulated (i.e., $\log_2$[fold change in expression] < −2) in the xylem of Line 3 compared to WT. Plots were assembled using Adobe Illustrator.

2.4 | Lignin Content, Composition, and Histology

Extractive-free cell wall material was obtained by extracting 40-mesh wood powder with hot acetone for 24 h in a Soxhlet apparatus. The total Klason lignin content was then determined using samples of extractive-free wood as the sum of acid-soluble and acid-insoluble fractions, and the composition of structural polysaccharides was measured by high-performance anion exchange chromatography of the hydrolysates, as described previously (Mottiar et al. 2023). Thioacidolysis reactions were then performed to evaluate the lignin composition, as described previously (Robinson and Mansfield 2009). Statistically significant differences between each line and the WT control were evaluated using a one-way ANOVA with a post hoc Dunnett's test conducted using SPSS Statistics 27 (IBM, Armonk, NY, USA).

Samples for NMR analysis were first ball-milled and treated with Cellulysin cellulase (from *Trichoderma viride*, Calbiochem, MilliporeSigma, Burlington, MA, USA) to prepare enzyme–lignin, which was then dissolved in 4:1 dimethyl sulphoxide-d_6:pyridine-d_5. Two-dimensional ^{1}H–^{13}C heteronuclear single-quantum coherence (2D-HSQC) NMR spectra were collected with a Biospin AVANCE 700 MHz spectrometer (Bruker Corp., Billerica, MA, USA), as described previously (Kim and Ralph 2010).

Transversal xylem cross-sections with a thickness of 10 μm were cut from the base of poplar stems using a sliding block microtome. Sections were stained with a 2:1 mixture of 3% phloroglucinol and concentrated hydrochloric acid and then imaged using a Reichert-Jung Polyvar microscope (Leica Microsystems, Wetzlar, Germany) equipped with an Olympus UC90 camera (Olympus Corp., Tokyo, Japan). The average number of vessels per 1000 × 1000-μm area was evaluated by examining 23 non-overlapping images representing over 100,000 cells for Line 3 (including more than 6000 vessels) and 31 images representing over 150,000 cells for WT (including more than 5000 vessels). Cell lumen areas were measured from the same images using an automated cell mapping and measurement pipeline with CellProfiler 4.1.3 (Carpenter et al. 2006).

2.5 | Metabolites

Frozen powders of developing xylem scrapings and young leaves were lyophilized overnight using a freeze dryer. Approximately 15 mg of dry material was extracted twice with 2.5 mL of 80% ethanol for 24 h. Prior to extraction, 75 μL of 1-mg mL^{-1} sorbitol was added as an internal standard. After combining the extracts, a 1-mL aliquot was dried under a stream of nitrogen and then derivatized by silylation. Trimethylsilylated derivatives were obtained by adding 500 μL each of acetonitrile and *N*-methyl-*N*-(trimethylsilyl)trifluoroacetamide containing 1% trimethylchlorosilane to the dried residue and then incubating for 1 h at 70°C. Samples were analyzed using an Agilent 7890A gas chromatograph (Agilent Technologies Inc., Santa Clara, CA, USA) equipped with an Rtx-5MS capillary column (5% diphenyl/95% dimethylpolysiloxane, 30 m × 250 μm, 0.25-μm film thickness, Restek Corp., Bellefonte, PA, USA) coupled to an Agilent 5975C inert XL mass spectrometer, as described previously (Tschaplinski et al. 2012). Metabolite concentrations were expressed as μg g^{-1} dry-weight material on a basis of sorbitol equivalents and then used to calculate the fold difference relative to WT control trees. Heat maps were assembled using Adobe Illustrator.

Methanolic extracts were obtained by incubating 10-mg samples of developing xylem in 80% methanol containing 1% acetic acid at 50°C in a hybridizer incubator for 3 h. Aliquots were then transferred into a fresh tube, the solvent was removed by evaporation in a vacuum centrifuge, an equal volume of 2 M HCl was added, and mild acid hydrolysis was conducted at 90°C for 2 h. The total amount of free salicylic acid (including that released from salicylic acid-containing glycosides) was then measured using an Agilent Infinity II 1290 UHPLC apparatus (Agilent Technologies Inc., Santa Clara, CA, USA) equipped with a Zorbax Eclipse Plus C-18 column (2.1 × 50 mm, 1.8-μm particle size, Agilent) and a diode array detector with the wavelength set to 304 nm. Good separation of peaks was achieved using an injection volume of 1 μL, a flow rate of 0.3 mL min^{-1}, and a binary gradient of 5%–30% of acetonitrile containing 0.01% trifluoroacetic acid (eluent A) in water containing 0.01% trifluoroacetic acid (eluent B) over 9 min.

3 | Results

3.1 | Identification of Poplar CM Isoforms

Amino acid sequences of the three CM isozymes from Arabidopsis were used to identify homologues in 14 diverse plant genomes. Among these taxa, there were as many as five isoforms per species (i.e., *Brassica rapa*) and as few as two (i.e., *Solanum tuberosum*, *Eucalyptus grandis*, and *Picea abies*). Maximum likelihood analysis of these putative CM sequences resulted in two major clades (Figure 2)—one containing *At*CM2, the cytosolic CM from Arabidopsis (shown in orange), and the other containing the two plastidic forms, *At*CM1 and *At*CM3 (shown in blue). In accordance with previously published structure-functional

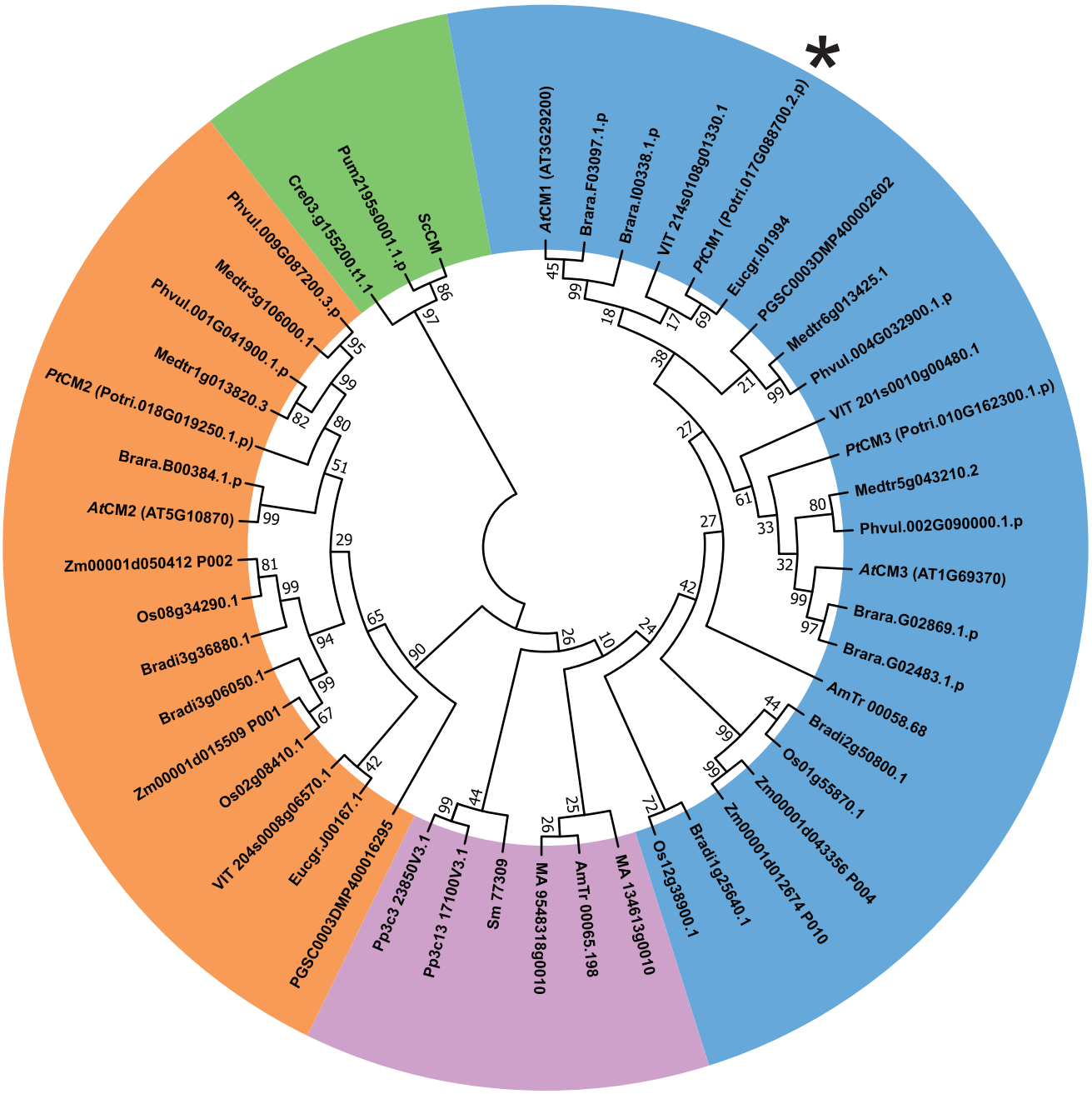

FIGURE 2 | Phylogenetic analysis of the chorismate mutase (CM) family. A maximum likelihood tree showing the relationships among the amino acid sequences of CM isoforms from diverse plant species including *Amborella trichopoda* (AmTr), *Arabidopsis thaliana* (AT), *Brachypodium distachyon* (Bradi), *Brassica rapa* (Brara), *Eucalyptus grandis* (Eucgr), *Medicago truncatula* (Medtr), *Oryza sativa* (Os), *Phaseolus vulgaris* (Phvu), *Physcomitrium patens* (Pp), *Picea abies* (MA), *Populus trichocarpa* (Potri), *Selaginella moellendorffii* (Sm), *Solanum tuberosum* (PGSC), *Vitis vinifera* (VIT), and *Zea mays* (Zm). The CM sequences from *Saccharomyces cerevisiae*, *Porphyra umbilicalis*, and *Chlamydomonas reinhardtii* were included as an outgroup (colored green). Putative cytosolic CM sequences are colored orange, plastidic CM sequences are colored blue, and the sequences from *S. moellendorffii*, *P. patens*, *P. abies*, and one of the sequences from *A. trichopoda* are colored purple. The values at each node represent statistical confidence based on 1000 bootstrap iterations. The asterisk denotes *Pt*CM1.

analyses (Westfall, Xu, and Jez 2014), nearly all the sequences in the plastidic cluster contained a glycine at position 148, which is necessary for allosteric regulation, with one exception from *Brachypodium distachyon* (Bradi1g25640.1). Conversely, all sequences in the *At*CM2-containing clade lacked this conserved glycine except for one sequence from *Vitis vinifera* (VIT 204s0008g06570.1). Interestingly, none of the CM sequences from *Physcomitrium patens*, *Selaginella moellendorffii*, *Picea abies*, or *Amborella trichopoda* contained this conserved residue, and these sequences predominantly clustered into a separate clade (shown in purple).

Three isoforms of CM were identified in the reference genome of poplar and were assigned names based on phylogeny and

sequence similarity with the Arabidopsis homologues. The poplar protein sequences were found to be 58%–62% identical to Arabidopsis (Figure S1A). Both *Pt*CM1 (Potri.017G088700) and *Pt*CM3 (Potri.010G162300) contain the conserved effector site glycine residue at positions 202 and 199, respectively, which confers allosteric sensitivity. There is also strong predictive support for the presence of plastid transit signals in both isoforms. In contrast, *Pt*CM2 (Potri.018G019250) lacks this conserved residue and shows no evidence of a plastid signal. The occurrence of glycine residues at positions 138 and 135 in *Pt*CM1 and *Pt*CM3 suggests that neither isoform exhibits the sensitivity to cysteine or histidine effectors that has been identified in *At*CM3 because of an aspartate residue at this position (Westfall, Xu, and Jez 2014). In short, *Pt*CM1 and *Pt*CM3 appear to be plastidic isoforms that are most likely allosterically activated by tryptophan and repressed by phenylalanine and tyrosine, whereas *Pt*CM2 appears to be cytosolic and unregulated.

3.2 | Downregulation of CM1 in Poplar

An RNAi-mediated approach was used to suppress the expression of *Pa*×*g*CM1, the orthologue of *Pt*CM1, in hybrid poplar (*Populus grandidentata*×*alba*; P39). Three independent transformants were selected for in-depth study (Figure 3A). As the three CM genes have relatively low sequence similarity to one another, it was possible to design a hairpin target specific for CM1 transcripts (Figure S1B, C). Although Lines 1 and 2 exhibited no major growth or developmental defects, Line 3 poplars were dwarfed compared to WT control trees (Figure 3B). All biological replicates of this line were consistently shorter in stature and thinner in stem diameter. Stunting is frequently observed as a response to perturbations in lignin production, often because of compromised vascular systems (Muro-Villanueva, Mao, and Chapple 2019). However, dwarfing can also result from myriad other metabolic or hormonal imbalances in plants (Bonawitz and Chapple 2013; Hollender and Dardick 2015). The leaves of Line 3 poplars were also small and showed obvious signs of chlorosis (Figure S2), even when grown under optimal conditions in tissue culture.

Gene expression analysis by RT-qPCR confirmed reduced expression of *Pa*×*g*CM1 transcripts in the xylem of all three lines (Figure 3C). Notably, in Line 3 poplars, *Pa*×*g*CM1 expression was decreased by 43%. Surprisingly, the expression of *Pa*×*g*CM2 and *Pa*×*g*CM3 was also altered. This was most pronounced in the developing xylem of Line 3, wherein the expression of *Pa*×*g*CM2 was more than doubled (i.e., an increase of 139%) and *Pa*×*g*CM3 expression was increased by more than 10-fold (i.e., an increase of 1094%). These unexpected observations suggest that the gene expression of CM paralogues can perhaps be modulated in compensation, at least in poplar xylem. The effects on gene expression in leaves were less clear, perhaps because of tissue-specific differences in transgene expression.

Given that severe dwarfing was observed only in Line 3, it is possible that this was due merely or even partially to the disruption of an endogenous gene in the poplar genome rather than solely misregulation of the target *Pa*×*g*CM1 gene. However, it

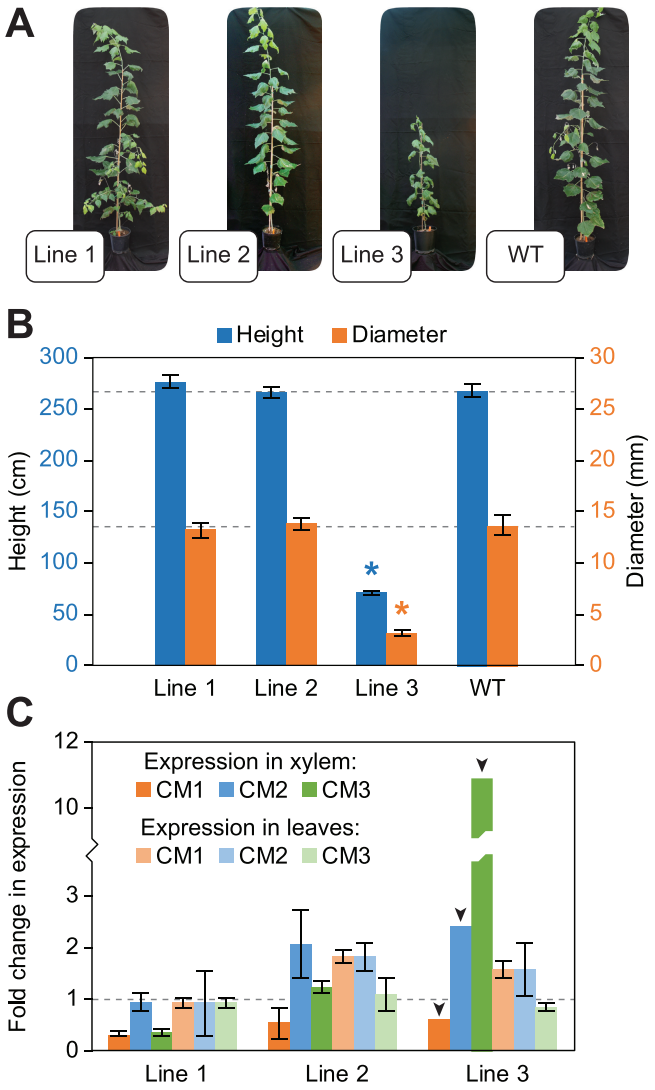

FIGURE 3 | RNAi-mediated suppression of CM1 in hybrid poplar trees. A: Representative photos of each line. B: Heights and diameters at the time of harvest. Error bars show standard deviation. The values marked with an asterisk are significantly different from the WT control, depicted with horizontal dashed lines (one-way ANOVA with Dunnett's test, $n=5$ for each line with technical triplicates, $p<0.05$). C: Fold change in expression of CM1, CM2, and CM3 in developing xylem and leaves relative to WT, normalized to the expression of elongation factor 1β. The horizontal dashed line represents no change in expression. The black arrowheads denote that error bars are not shown for the xylem of Line 3 because the biological replicates were pooled and analyzed in triplicate because of limited samples. Otherwise, three biological replicates were analyzed in triplicate for each line. Note the break in the *y*-axis.

is also plausible that Line 3 was simply the most impacted of the three lines. It could also be that this variation resulted from differences in the number of transgene insertion events, or the position of the insertions.

It is worth emphasizing that, because of sample limitations resulting from the poor growth of Line 3 trees, many of the following analyses were performed on pooled samples. For this reason, it is not possible to perform meaningful statistical analyses for Line 3 in those experiments. Nonetheless, the results are

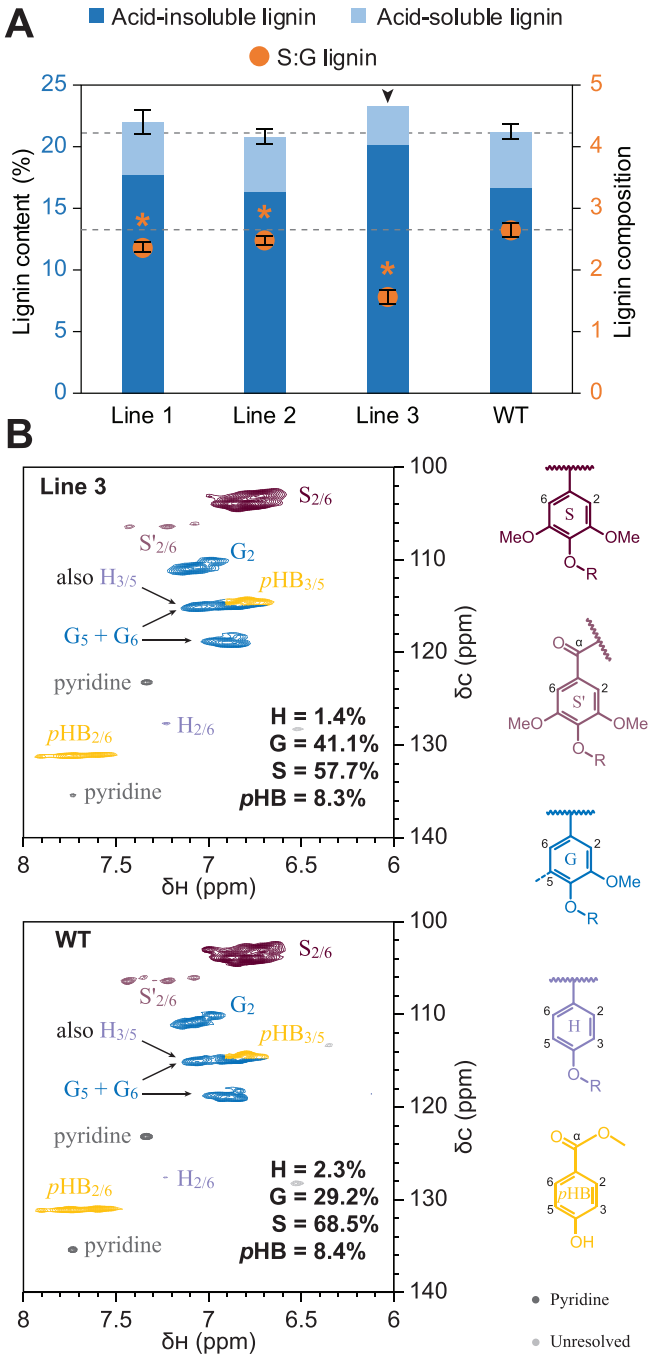

FIGURE 4 | Legend on next page.

FIGURE 4 | Lignin analysis of *Pa*×*g*CM1 RNAi poplar trees. A: Klason lignin content was measured as the sum of acid-insoluble and acid-soluble fractions and is plotted on the left axis in blue. The ratio of syringyl (S): guaiacyl (G) lignin monomers was evaluated by thioacidolysis and is plotted on the right axis in orange. Five biological replicates were analyzed in triplicate for each line and the error bars show standard deviation, except for Line 3 wherein the biological replicates were pooled and analyzed in triplicate because of limited samples (denoted with a black arrowhead). The values marked with an asterisk are significantly different from the wild-type (WT) control, depicted with horizontal dashed lines (one-way ANOVA with Dunnett's test, $n = 5$ for each line with technical triplicates, p-value < 0.05). B: Partial two-dimensional ^{1}H–^{13}C HSQC NMR spectra for enzyme–lignin samples of Line 3 and the WT control, as labeled, showing the aromatics region. The spectra are representative of technical repeats, but no statistical analyses were performed. The color-coding and peak annotations for *p*-hydroxyphenyl (H, light purple), guaiacyl (G, blue), and syringyl units (S and S′, dark and light magenta), as well as *p*-hydroxybenzoate pendent groups (yellow, *p*HB) are elaborated with the structures shown on the side. Percentages are expressed on a basis where H + G + S = 100%.

provided to identify possible trends and illustrate the potential impacts of CM1 suppression in poplar.

3.3 | Compensatory Lignification in CM1-Suppressed Poplar

To examine how the reduced expression of *Pa*×*g*CM1 affected xylem lignification, the lignin content, and composition of mature wood were examined next. Rather than a decrease in lignin content, which might have been expected, Line 3 exhibited a 10% increase in the total amount of lignin compared to WT (Figure 4A), likely resulting from the compensatory expression of *Pa*×*g*CM2 and *Pa*×*g*CM3. This change in lignin content was accompanied by an increase in the proportion of G-lignin units measured by thioacidolysis (i.e., decreased S:G lignin ratio; Figure 4A). Although there were no significant differences in the total lignin contents of Lines 1 and 2 compared to the WT control, these lines also had an increased G-lignin content, as was observed in Line 3. This observation supports the view that Line 3 represents an extreme example of a trend rather than an anomaly. The shift toward coniferyl alcohol-derived G-lignin units could be a result of altered flux through the phenylpropanoid pathway, consistent with previous reports on transgenic poplars (Wang et al. 2019). An analysis of the structural polysaccharides also revealed minor differences in composition (Table S2), although these were not consistent across the different transgenic lines.

Analysis by 2D-HSQC NMR confirmed the shift in lignin composition toward G-lignin units and revealed a small decrease in H-lignin (Figure 4B). Despite the change in monomer composition, there was no significant difference in the proportion of *p*-hydroxybenzoate groups. These ester-linked pendent moieties occur naturally in the lignin of poplar, and their abundance can change in response to altered flux through the phenylpropanoid pathway (Goacher, Mottiar, and Mansfield 2021; Mottiar et al. 2023). Further examination of the NMR spectra showed that there were also minor decreases in the proportions of β-aryl ether, resinol, and tetrahydrofuran linkages, as well as an increase in phenylcoumaran structures (Figure S3), likely because of the greater abundance of G-lignin units.

Next, transversal stem cross-sections were examined by light microscopy to ascertain whether there were changes in xylem development. Staining with phloroglucinol–HCl revealed marked differences in xylem morphology between Line 3 and the WT control, namely, an increase in the number of vessels and a decrease in the average vessel lumen area (Figure 5). Despite these differences in vessel density and lumen size, irregularly shaped vessels were not observed and the vascular

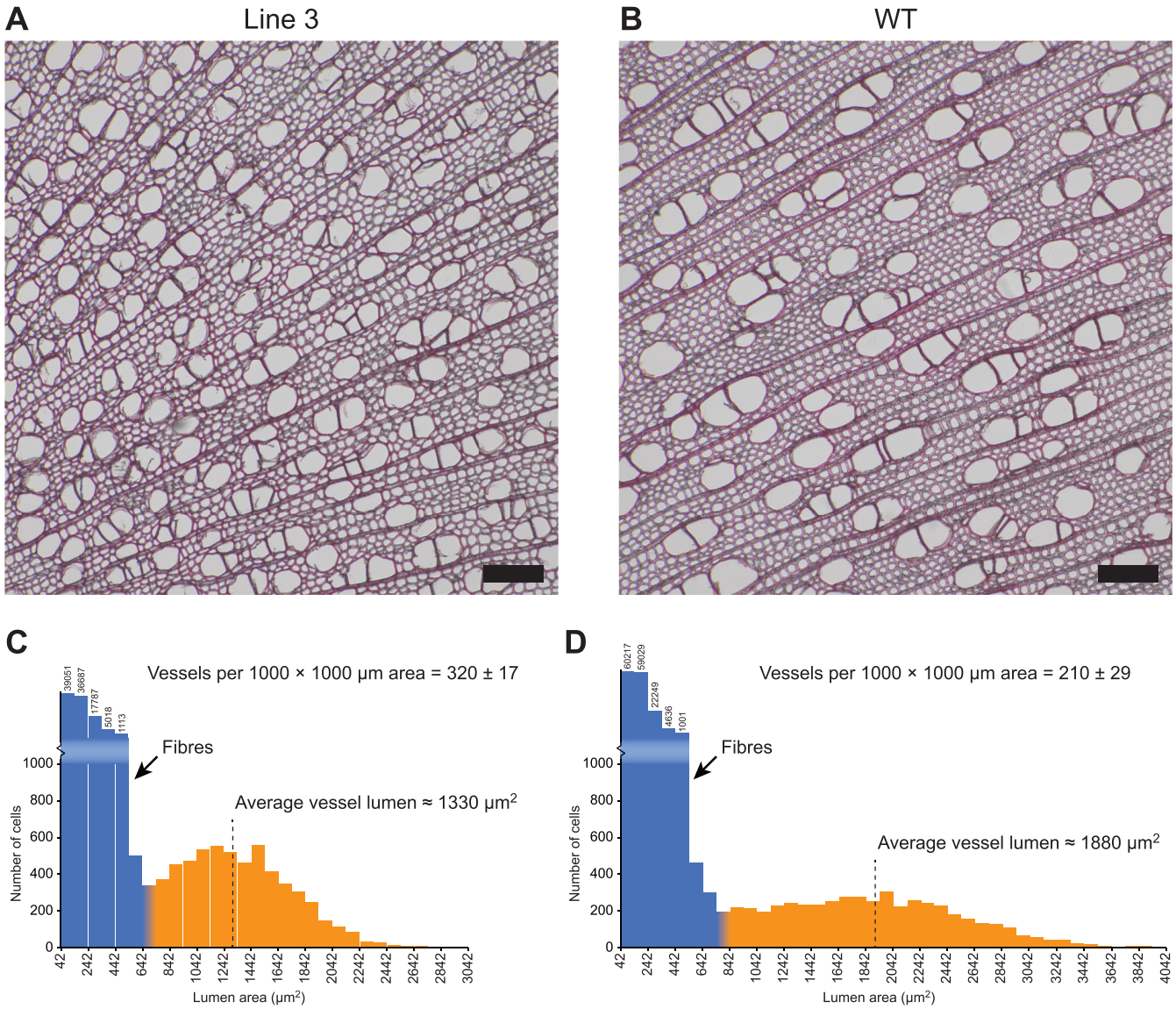

FIGURE 5 | Lignin histology of *Pa*×*g*CM1 RNAi poplar trees. Transversal xylem cross-sections of Line 3 (A) and WT (B) poplar stems, as labeled, stained with phloroglucinol–HCl. The black scale bars represent 100 µm. Histograms for Line 3 (C) and WT (D) showing the distribution of cell lumen areas with fibers shown in blue and vessels in orange.

system appeared to be properly formed. Moreover, there were no obvious differences in the intensity of lignin staining. Accordingly, it is unlikely that stunting of Line 3 is a direct consequence of lignin perturbation and impaired water conduction, but it could instead be a sign of more far-reaching metabolic stresses.

Increased vessel density may partially help explain the elevated levels of guaiacyl units observed in Line 3 xylem, as poplar vessels are known to be enriched in G lignin (Musha and Goring 1975). However, a corresponding decrease in lignin-associated *p*-hydroxybenzoate would also have been expected as these groups are normally restricted to fiber cell walls (Goacher, Mottiar, and Mansfield 2021; Mottiar and Mansfield 2022). Therefore, the observation that *p*-hydroxybenzoate levels remained unchanged in Line 3 provides further evidence of altered carbon flux through the phenylpropanoid pathway.

3.4 | Systemic Responses in Plant Metabolism

Next, we examined whether the perturbations in lignin biosynthesis were accompanied by more widespread changes in metabolism. Gas chromatography coupled with mass spectrometry was used to quantify an array of metabolites including amino acids and soluble phenolics. The levels of all amino acids detected were reduced in the developing xylem of all lines compared to WT with Line 3 again being the most drastically altered (Figure 6A). Histidine, aspartate, and tryptophan were especially deficient in the xylem of Line 3. Metabolic profiling of young leaves also showed reductions in various amino acids, with the exception of glycine which was more abundant in Line 3 compared to WT (Figure 6C). In general, the observed differences in leaf metabolites between WT and *Pa*×*g*CM1-suppressed poplar were less extreme than the variation observed in developing xylem, perhaps reflecting the more modest differences in gene expression in leaves. Free amino acids are broadly involved

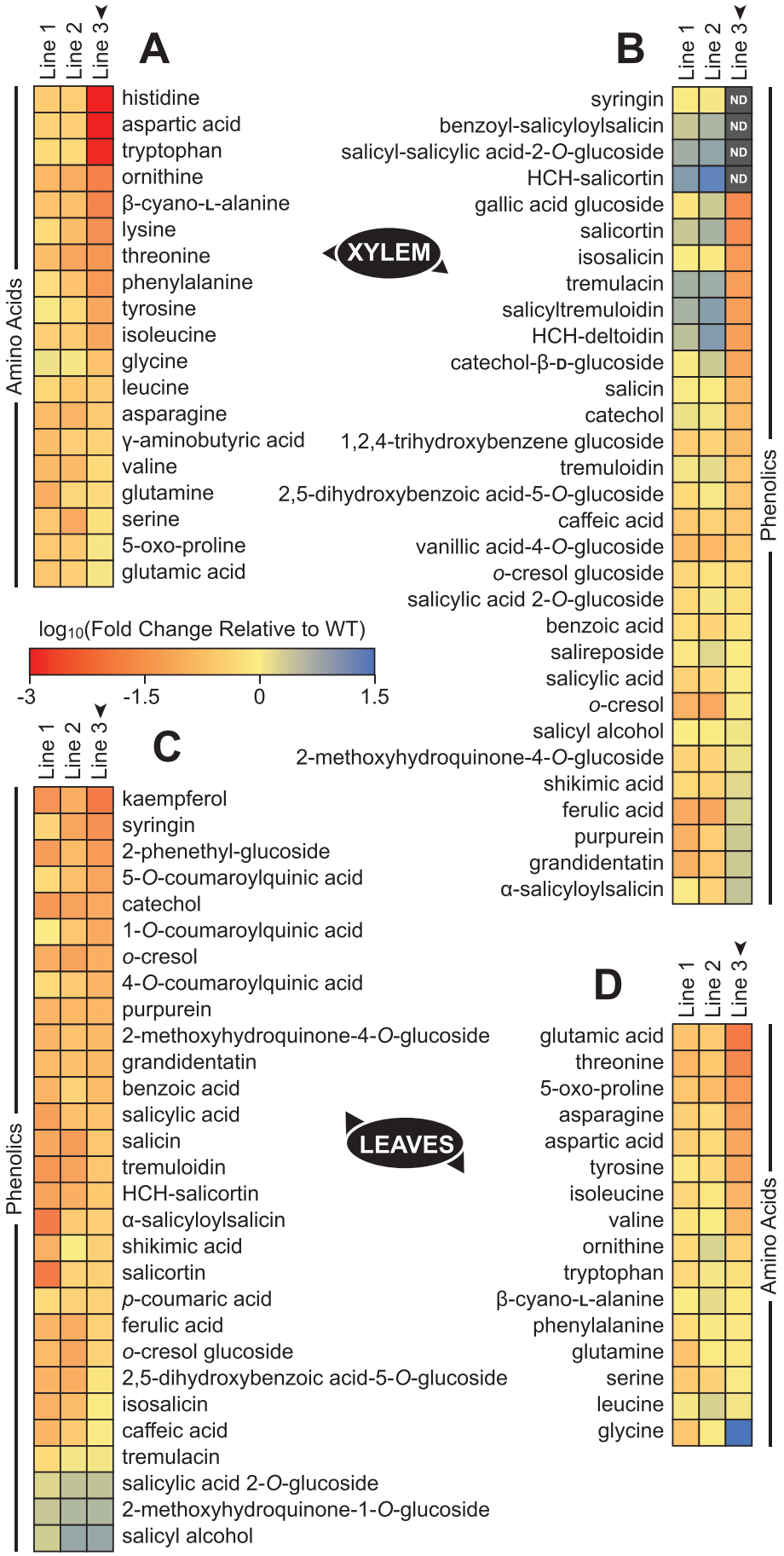

FIGURE 6 | Legend on next page.

FIGURE 6 | Metabolite profiling of *Pa*×*g*CM1 RNAi poplar trees. A, B: Heat maps depicting the log of the fold change in the levels of 19 amino acids and 31 phenolic compounds in the developing xylem of Lines 1–3 relative to the wild-type (WT) control, as labeled. C, D: Heat maps depicting the log of the fold change in the levels of 29 phenolic compounds and 16 amino acids in the young leaves of Lines 1–3 relative to WT, as labeled. The color gradient bar shows that red and orange correspond to negative values (i.e., a decrease relative to WT), whereas blue corresponds to positive values (i.e., an increase relative to WT). Gray squares labeled ND indicate that several metabolites were not detected in Line 3. The black arrowheads denote that biological replicates of developing xylem were pooled for Line 3 because of limited samples. Otherwise, five biological replicates were analyzed for each line. No statistical analyses were performed on this dataset.

in modulating stress responses, membrane permeability, and ion uptake (Barneix and Causin 1996; Rai 2002). The reduced levels in *Pa*×*g*CM1-suppressed poplar could be an indication that one or more of these processes have been affected. However, there is no obvious explanation for the increased glycine in leaves. Interestingly, there was no hyperaccumulation of asparagine which is sometimes observed following biotic and abiotic stress (Anzano et al. 2022), suggesting that CM1 disruption may provoke a unique metabolic response.

The abundance of many phenolic compounds was also altered in the developing xylem and young leaves of Line 3 (Figure 6B,D). For example, syringin, a glucoside of sinapyl alcohol, was reduced below detection levels in the xylem. This observation is consistent with the observed reduction in S-lignin units evidenced by thioacidolysis and NMR and could be related to the increased proportion of G-lignin-rich vessel elements. Coniferin, the glucoside of coniferyl alcohol, was however not detected either in WT or transgenic samples. Several salicylic acid derivatives were drastically reduced, perhaps a result of perturbations in the pool of salicylic acid, which is also derived from chorismate. Interestingly, several of these compounds were actually more abundant in Lines 1 and 2, wherein the compensatory expression of *Pa*×*g*CM2 and *Pa*×*g*CM3 was evidently lower as there were no obvious impacts on growth and development. In the Salicaceae family, which includes poplar, salicinoid metabolites are known to occur naturally as defensive compounds (Boeckler, Gershenzon, and Unsicker 2011). More broadly, free salicylic acid plays a role in regulating plant growth and development, photosynthesis, ion uptake and transport, and responses to biotic and abiotic stress (Vicente and Plasencia 2011). Further analysis of the soluble phenolics by UHPLC confirmed that the developing xylem of Line 3 poplars contained drastically reduced total amounts of salicylic acid, which was liberated from salicylic acid–containing metabolites by mild acid hydrolysis (Figure S4).

In addition to free amino acids and phenolics, metabolite profiling revealed widespread changes in the occurrence of various organic acids (Figure S5A,C). Several of these metabolites were decreased in Lines 1 and 2 but elevated in Line 3. Organic acids play an important role in various processes, but, perhaps most notably, they help maintain the redox balance of reactive oxygen species in plants that result from photosynthesis and cellular respiration (Igamberdiev and Bykova 2018). Other metabolites including some sugars, sugar alcohols, and sterols were also decreased in the *Pa*×*g*CM1-suppressed lines (Figure S5B,D). These observations show that widespread changes in metabolic processes occurred as a result of *Pa*×*g*CM1 misregulation and may provide some additional clues as to why Line 3 was stunted and chlorotic. Of course, it is also plausible that these metabolic changes were due to the observed increased expression of *Pa*×*g*CM2 and *Pa*×*g*CM3 rather than specifically the decreased expression of *Pa*×*g*CM1.

3.5 | Perturbations in Gene Expression

To further resolve the systemic responses in *Pa*×*g*CM1-suppressed poplar, RNA-seq experiments were performed to compare the gene expression profiles of the developing xylem in Line 3 to the WT control (Table S3). This analysis corroborated the previous gene expression analysis which showed a downregulation of *Pa*×*g*CM1 in Line 3 coincident with an increase in the expression of *Pa*×*g*CM2 and *Pa*×*g*CM3. Furthermore, an enrichment analysis of GO terms revealed that many of the differentially expressed genes were involved in photosynthesis, ion binding, and redox processes (Figure S6). These results provide further evidence that suppression of *Pa*×*g*CM1 had widespread consequences beyond merely affecting the biosynthesis of lignin and phenylpropanoids.

Finally, the expression of shikimate and phenylpropanoid pathway genes was examined in Line 3 relative to the WT control. Most genes in the shikimate pathway were downregulated with the exception of one isoform for each of 3-deoxy-d-arabino-heptulosonate 7-phosphate synthase, chorismate synthase, arogenate dehydratase, and arogenate dehydrogenase (Table S4). Similarly, most genes in the phenylpropanoid pathway were downregulated except for several isoforms of phenylalanine ammonia lyase, and one isoform each of 4-coumarate CoA ligase and *p*-coumaroyl-shikimate/quinate-3-hydroxylase (Table S5). It could be that this reflects a partial upregulation of the pathway leading to lignin formation specifically in response to a reduction of *Pa*×*g*CM1 activity in Line 3 plants. It could also reflect a temporal shift in gene expression resulting from premature lignification or other developmental changes. Alternatively, the observed changes in gene expression could be merely a reflection of a more widespread stress response.

4 | Discussion

4.1 | Parallel Routes Through the Shikimate Pathway

In this study, we interrogated the role of *Pa*×*g*CM1 by suppressing its expression in hybrid poplar. In addition to being the most highly expressed isoform in the developing xylem of poplar, *Pa*×*g*CM1 is predicted to be plastidic and allosterically regulated (Westfall, Xu, and Jez 2014). It has long been assumed that carbon destined for lignin biosynthesis is generated via the

plastid-localized shikimate pathway, particularly given the vast amounts of photosynthetic carbon that must be allocated to lignin production in developing xylem (Pinard and Mizrachi 2018). Moreover, the existence of a cytosolic shikimate pathway had been frequently contested and was only definitely demonstrated recently (Qian et al. 2019; Lynch 2022).

It may be that the cytosolic route is specifically employed in the production of non-lignin metabolites. But even still, metabolic flux through the cytosolic pathway could play an important role in regulating lignin biosynthesis, which occurs in the cytosol, since esters of shikimate are needed for phenylpropanoid biosynthesis beyond *p*-coumaroyl-CoA (Adams, Ehlting, and Edwards 2019). The observation that *Pa*×*g*CM2 was upregulated in *Pa*×*g*CM1-suppressed poplar suggests that there may be at least some interplay between the cytosolic and plastidic branches of the shikimate pathway and that even the allosterically insensitive isoform can be enlisted for lignin precursor biosynthesis. However, the apparent pleiotropic effects on plant growth and metabolism indicate that the parallel routes of the shikimate pathway may not be fully interchangeable.

Given that the shikimate pathway gives rise to a wide variety of primary and secondary metabolites alike, it comes as no surprise that perturbations can have widespread and sometimes unexpected consequences in plants. For example, overexpression of the cytosolic CM2 in petunia ultimately led to a decrease in phenylalanine and phenylalanine-derived floral volatiles rather than an increase because of elevated production of indole-derived auxin (Lynch 2022). This also vividly illustrates the important crosstalk that can occur between the various metabolic pathways that lie downstream of chorismate, particularly when perturbations are pushed to extremes.

Nonetheless, manipulation of shikimate pathway intermediates leading to lignin can be permissible in poplar if it is spatiotemporally restricted by using secondary cell wall-specific promoters to drive expression. For example, the introduction of a shikimate kinase was successfully used to manipulate the cytosolic levels of shikimate and thereby impact the biosynthesis and structure of lignin (Hu et al. 2022). Similarly, heterologous expression of bacterial enzymes in the plastid has been used to divert carbon flux away from the shikimate pathway for the purposes of engineering the content, composition, and structure of lignin (Unda et al. 2022; Mottiar et al. 2023).

4.2 | Chorismate Is a Pivotal Branchpoint Metabolite

Suppression of *Pa*×*g*CM1, and the corresponding increased expression of *Pa*×*g*CM2 and *Pa*×*g*CM3, led to changes in various free amino acids, soluble phenolics, and organic acids in the young leaves and developing xylem of poplar. These metabolites play important roles in a variety of processes in plants including redox homeostasis, ion uptake and binding, and stress responses. Interestingly, many of the same metabolite classes that were depleted in Line 3 were reportedly elevated in the aerial tissues of Arabidopsis when an allosterically insensitive CM was overexpressed (Tzin et al. 2009). Widespread changes in the metabolite profiles of flowers were also observed when chorismate synthase was suppressed in petunia (Zhong et al. 2020), further illustrating the importance of chorismate as a key metabolic branchpoint.

The observation that lignin content was elevated in Line 3 relative to WT suggests that compensatory expression of *Pa*×*g*CM2 and *Pa*×*g*CM3 was evidently more than sufficient to satisfy the demand for chorismate during xylem lignification. However, the apparent oversupply of lignin precursors may be a sign that chorismate formation driven by *Pa*×*g*CM2 and *Pa*×*g*CM3 was not adequately controlled. This could be related to differences in allosteric regulation or subcellular localization, or it might simply be a consequence of timing. Typically, lignin formation is tightly controlled at multiple levels so that monolignol biosynthesis, export, and polymerization occur at the appropriate spatial and temporal juncture during programmed cell death (Donaldson 2001; Boerjan, Ralph, and Baucher 2003; Bollhöner, Prestele, and Tuominen 2012).

It is likely that the stunting observed with Line 3 trees was not merely a consequence of changes in lignin biosynthesis or phenylpropanoid metabolism. Allocation of carbon toward lignin biosynthesis via *Pa*×*g*CM2 and *Pa*×*g*CM3 rather than *Pa*×*g*CM1 may have led to perturbations in the pool of salicylic acid. A severe dwarfing phenotype was reported when salicylic acid hyperaccumulated in transgenic Arabidopsis (Mauch et al. 2001). On the other hand, salicylic acid accumulation led to oxidative stress, but not stunting in poplar (Xue et al. 2013). Additional studies have also shown that metabolic connections exist between CM activity and salicylic acid levels. For example, salicylic acid levels produced in response to biotic stress were increased when CM was overexpressed in transgenic rice (Jan et al. 2021). Inversely, CM was downregulated in tobacco plants when salicylic acid levels were constitutively elevated (Nugroho, Verberne, and Verpoorte 2002). Various fungal pathogens and parasitic nematodes have exploited this metabolic connection by secreting a CM enzyme which they likely acquired via horizontal gene transfer in order to compromise plant defense systems by manipulating salicylic acid levels in host tissues (Lambert, Allen, and Sussex 1999; Djamei et al. 2011).

4.3 | Potential Redundancy in the CM Gene Family

Few studies have considered whether CM isoforms have distinct or overlapping roles in plants despite the importance of this gene family in both primary and secondary metabolism. Transcriptome databases for Arabidopsis and poplar show that *At*CM2 and *Pt*CM2 (the cytosolic and allosterically insensitive isoforms) are constitutively expressed, whereas the other isoforms have partially overlapping expression profiles in various organs and tissues (Waese et al. 2017; Sundell et al. 2015; Sundell et al. 2017; Figure S7). The observation that RNAi-mediated suppression of *Pa*×*g*CM1 did not result in decreased lignin biosynthesis suggests that at least partial redundancy may occur within the poplar CM gene family. It may also be that CM homologues are differentially expressed as a response to stress. Interestingly, both the unregulated and regulated isoforms (*Pa*×*g*CM2 and *Pa*×*g*CM3) showed elevated expression

in response to the suppression of *Pa*×*g*CM1 in the developing xylem of Line 3.

A major limitation of this study is that only one of the three RNAi transgenic lines had a significant difference in lignin content (although all three lines had differences in lignin composition). Moreover, this was also the only line with obvious growth and developmental phenotypes. Although we cannot exclude the possibility that differences in the number and location of transgene insertions could be confounding factors, it is apparent that Line 3 was the only line with sufficient effects on the shikimate pathway to produce severe phenotypes and elicit significant compensatory expression of the other CM isoforms as well as an array of other genes in the shikimate and phenylpropanoid pathways. The two other RNAi lines may have been affected but to a lesser degree. Indeed, all three transgenic lines exhibited differences in a wide array of metabolites, including various phenolic derivatives of the shikimate pathway. However, the impacts of *Pa*×*g*CM1 suppression on gene expression in the leaf tissues were less clear than in the xylem. Additional transgenic experiments would certainly be needed to confirm that the CM gene family is functionally redundant in poplar.

At present, it remains unclear whether any functional redundancy extends beyond the metabolic requirements for chorismate to supply lignin biosynthesis in developing xylem tissues. It would be a worthwhile future experiment to specifically knock down the other two CM isoforms in poplar to see if *Pa*×*g*CM1 is upregulated and to ascertain whether compensatory expression can be reciprocal. It may be worthwhile employing activation targeting, CRISPR, and other techniques for this pursuit. It is also unknown how broadly CM gene redundancy might occur across different plant taxa. For example, in petunia, RNAi-mediated suppression of CM1 was accompanied by a reduction in the biosynthesis of volatile phenolic compounds in flowers but was not associated with increased expression of any other isoforms (Colquhoun et al. 2010), suggesting that CM redundancy may not be universal. Thus, further mutant and transgenic studies in diverse plant species will be needed to resolve this question. As the phylogenetic analysis showed that some taxa evidently contain as many as five CM isoforms, these could be particularly informative species for future studies.

In summary, this work highlights the central role of chorismate as a key precursor to a wide range of important plant metabolites. Compensatory expression of potentially redundant CM isoforms in *Pa*×*g*CM1-misregulated hybrid poplar was accompanied by widespread changes in gene expression and metabolism which affected photosynthesis, ion transport, and redox processes, as well as plant growth and xylem development. These systemic responses may have been the result of perturbations in the biosynthesis of salicylic acid, as this too derives from chorismate. However, many of the observed effects were only apparent in a single transgenic line. If indeed some level of gene redundancy occurs broadly within the CM gene family, this is most certainly a consequence of the critically important position that chorismate occupies at the junction of a series of important biosynthetic pathways in plants.

Author Contributions

Y.M. and S.D.M. devised the research project, T.J.T. completed the analysis of metabolites, J.R. helped with the NMR analysis, and Y.M. performed all the other experiments. Y.M. wrote the manuscript, and all authors contributed to the final version.

Acknowledgments

Financial support for this work was provided by a Korea Institute of Science and Technology grant to S.D.M. by the Great Lakes Bioenergy Research Center, U.S. Department of Energy, Office of Science, Office of Biological and Environmental Research, under Award Number DE-SC0018409 to S.D.M. and J.R., and by the Center for Bioenergy Innovation, U.S. Department of Energy, Office of Science, Office of Biological and Environmental Research, under Award Number FWP ERKP886 to T.J.T. This manuscript has been supported by UT-Battelle LLC, under Contract No. DE-AC05-00OR22725 with the U.S. Department of Energy. We also gratefully acknowledge the help of Kaye A. Hare with plant maintenance, photography, and harvesting; Charles Hefer with preprocessing of the RNA-seq data; and Nancy L. Engle, Madhavi Z. Martin, and Audrey D. Labbé with the untargeted analysis of metabolites.

References

Adams, Z. P., J. Ehlting, and R. Edwards. 2019. "The Regulatory Role of Shikimate in Plant Phenylalanine Metabolism." *Journal of Theoretical Biology* 462: 158–170.

Amthor, J. S. 2003. "Efficiency of Lignin Biosynthesis: A Quantitative Analysis." *Annals of Botany* 91, no. 6: 673–695.

Anzano, A., G. Bonanomi, S. Mazzoleni, and V. Lanzotti. 2022. "Plant Metabolomics in Biotic and Abiotic Stress: A Critical Overview." *Phytochemistry Reviews* 21: 503–524.

Armenteros, J. J. A., M. Salvatore, O. Emanuelsson, et al. 2019. "Detecting Sequence Signals in Targeting Peptides Using Deep Learning." *Life Science Alliance* 2, no. 5: e201900429.

Ball, S. G., R. B. Wickner, G. Cottarel, M. Schaus, and C. Tirtiaux. 1986. "Molecular Cloning and Characterization of *ARO7-OSM2*, a Single Yeast Gene Necessary for Chorismate Mutase Activity and Growth in Hypertonic Medium." *Molecular & General Genetics* 205, no. 2: 326–330.

Barneix, A. J., and H. F. Causin. 1996. "The Central Role of Amino Acids on Nitrogen Utilization and Plant Growth." *Journal of Plant Physiology* 149, no. 3–4: 358–362.

Behr, M., G. Guerriero, J. Grima-Pettenati, and M. Baucher. 2019. "A Molecular Blueprint of Lignin Repression." *Trends in Plant Science* 24, no. 11: 1052–1064.

Boeckler, G. A., J. Gershenzon, and S. B. Unsicker. 2011. "Phenolic Glycosides of the Salicaceae and Their Role as Anti-Herbivore Defenses." *Phytochemistry* 72, no. 13: 1497–1509.

Boerjan, W., J. Ralph, and M. Baucher. 2003. "Lignin Biosynthesis." *Annual Review of Plant Biology* 54: 519–546.

Bollhöner, B., J. Prestele, and H. Tuominen. 2012. "Xylem Cell Death: Emerging Understanding of Regulation and Function." *Journal of Experimental Botany* 63, no. 3: 1081–1094.

Bonawitz, N. D., and C. Chapple. 2013. "Can Genetic Engineering of Lignin Deposition Be Accomplished Without an Unacceptable Yield Penalty?" *Current Opinion in Biotechnology* 24: 336–343.

Bonner, C.A., andR.A. Jensen. 1998. Upstream Metabolic Segments That Support Lignin Biosynthesis. In: *Lignin and Lignan Biosynthesis.* ACS Symposium Series, Eds.NG Lewis, S Sarkanen, 697, 29–41. American Chemical Society, Washington, DC, USA.

Bowsher, C., M. Steer, and A. Tobin. 2008. *Plant Biochemistry*. Taylor & Francis Group New York, USA.

Carpenter, A. E., T. R. Jones, M. R. Lamprecht, et al. 2006. "CellProfiler: Image Analysis Software for Identifying and Quantifying Cell Phenotypes." *Genome Biology* 7, no. 1: R100.

Cass, C. L., A. Peraldi, P. F. Dowd, et al. 2015. "Effects of PHENYLALANINE AMMONIA LYASE (PAL) Knockdown on Cell Wall Composition, Biomass Digestibility, and Biotic and Abiotic Stress Responses in Brachypodium." *Journal of Experimental Botany* 66, no. 14: 4317–4335.

Colquhoun, T. A., B. C. J. Schimmel, J. Y. Kim, D. Reinhardt, K. Cline, and D. G. Clark. 2010. "A Petunia Chorismate Mutase Specialized for the Production of Floral Volatiles." *Plant Journal* 61, no. 1: 145–155.

d'Amato, T. A., R. J. Ganson, C. G. Gaines, and R. A. Jensen. 1984. "Subcellular Localization of Chorismate-Mutase Isoenzymes in Protoplasts From Mesophyll and Suspension-Cultured Cells of *Nicotiana silvestris*." *Planta* 162, no. 2: 104–108.

Djamei, A., K. Schipper, F. Rabe, et al. 2011. "Metabolic Priming by a Secreted Fungal Effector." *Nature* 478, no. 7369: 395–398.

Donaldson, L. A. 2001. "Lignification and Lignin Topochemistry: An Ultrastructural View." *Phytochemistry* 57, no. 6: 859–873.

Eberhard, J., T. T. Ehrler, P. Epple, et al. 1996. "Cytosolic and Plastidic Chorismate Mutase Isozymes From *Arabidopsis thaliana*: Molecular Characterisation and Enzymatic Properties." *Plant Journal* 10, no. 5: 815–821.

Eberhard, J., H.-R. Raesecke, J. Schmid, and N. Amrhein. 1993. "Cloning and Expression in Yeast of a Higher Plant Chorismate Mutase: Molecular Cloning, Sequencing of the cDNA and Characterization of the *Arabidopsis thaliana* Enzyme Expressed in Yeast." *FEBS Journal* 334, no. 2: 233–236.

Ehlting, J., N. Matteus, D. S. Aeschliman, et al. 2005. "Global Transcript Profiling of Primary Stems From *Arabidopsis thaliana* Identifies Candidate Genes for Missing Links in Lignin Biosynthesis and Transcriptional Regulators of Fiber Differentiation." *Plant Journal* 42, no. 5: 618–640.

Gibson, L. J. 2012. "The Hierarchical Structure and Mechanics of Plant Materials." *Journal of the Royal Society Interface* 9: 2749–2766.

Goacher, R. E., Y. Mottiar, and S. D. Mansfield. 2021. "ToF-SIMS Imaging Reveals That *p*-Hydroxybenzoate Groups Specifically Decorate the Lignin of Fibres in the Xylem of Poplar and Willow." *Holzforschung* 75, no. 5: 452–462.

Gorisch, H. 1978. "On the Mechanism of the Chorismate Mutase Reaction." *Biochemistry* 17, no. 18: 3700–3705.

Helliwell, C., and P. Waterhouse. 2003. "Constructs and Methods for High-Throughput Gene Silencing in Plants." *Methods* 30, no. 4: 289–295.

Herrmann, K. M. 1995. "The Shikimate Pathway: Early Steps in the Biosynthesis of Aromatic Compounds." *Plant Cell* 7, no. 7: 907–919.

Hollender, C. A., and C. Dardick. 2015. "Molecular Basis of Angiosperm Tree Architecture." *New Phytologist* 206, no. 2: 541–556.

Hu, S., N. Kamimura, S. Sakamoto, et al. 2022. "Rerouting of the Lignin Biosynthetic Pathway by Inhibition of Cytosolic Shikimate Recycling in Transgenic Hybrid Aspen." *Plant Journal* 110, no. 2: 358–376.

Huang, X., C. A. Hefer, R. Y. Soolanayakanahally, R. D. Guy, and S. D. Mansfield. 2024. "The Overlooked Ion: Unraveling the Effects of Magnesium-Specific Toxicity on Willows Under Sulphate Salinity." *Environmental and Experimental Botany* 219: 105634.

Igamberdiev, A. U., and N. V. Bykova. 2018. "Role of Organic Acids in the Integration of Cellular Redox Metabolism and Mediation of Redox Signalling in Photosynthetic Tissues of Higher Plants." *Free Radical Biology and Medicine* 122: 74–85.

Jan, R., M. A. Khan, S. Asaf, Lubna, I.-J. Lee, and K.-M. Kim. 2021. "Over-Expression of Chorismate Mutase Enhances the Accumulation of Salicylic Acid, Lignin, and Antioxidants in Response to the White-Backed Planthopper in Rice Plants." *Antioxidants* 10, no. 11: 1680.

Kim, H., and J. Ralph. 2010. "Solution-State 2D NMR of Ball-Milled Plant Cell Wall Gels in DMSO-d_6/Pyridine-d_5." *Organic & Biomolecular Chemistry* 8, no. 3: 576–591.

Kolosova, N., B. Miller, S. Ralph, et al. 2004. "Isolation of High-Quality RNA From Gymnosperm and Angiosperm Trees." *BioTechniques* 36, no. 5: 821–824.

Kumar, S., G. Stecher, M. Li, C. Knyaz, and K. Tamura. 2018. "MEGA X: Molecular Evolutionary Genetics Analysis Across Computing Platforms." *Molecular Biology and Evolution* 35, no. 6: 1547–1549.

Lambert, K. N., K. D. Allen, and I. M. Sussex. 1999. "Cloning and Characterization of an Esophageal-Gland-Specific Chorismate Mutase From the Phytoparasitic Nematode *Meloidogyne Javanica*." *Molecular Plant-Microbe Interactions* 12, no. 4: 328–336.

Li, M., Y. Pu, and A. J. Ragauskas. 2016. "Current Understanding of the Correlation of Lignin Structure With Biomass Recalcitrance." *Frontiers in Chemistry* 4: 45.

Lynch, J. H. 2022. "Revisiting the Dual Pathway Hypothesis of Chorismate Production in Plants." *Horticulture Research* 9: uhac052.

Maeda, H., and N. Dudareva. 2012. "The Shikimate Pathway and Aromatic Amino Acid Biosynthesis in Plants." *Annual Review of Plant Biology* 63: 73–105.

Mauch, F., B. Mauch-Mani, C. Gaille, B. Kull, D. Haas, and C. Reimmann. 2001. "Manipulation of Salicylate Content in *Arabidopsis thaliana* by the Expression of an Engineered Bacterial Salicylate Synthase." *Plant Journal* 25, no. 1: 67–77.

Miedes, E., R. Vanholme, W. Boerjan, and A. Molina. 2014. "The Role of the Secondary Cell Wall in Plant Resistance to Pathogens." *Frontiers in Plant Science* 5: 358.

Mobley, E. M., B. N. Kunkel, and B. Keith. 1999. "Identification, Characterization and Comparative Analysis of a Novel Chorismate Mutase Gene in *Arabidopsis thaliana*." *Gene* 240, no. 1: 115–123.

Mottiar, Y., N. Gierlinger, D. Jeremic, E. R. Master, and S. D. Mansfield. 2020. "Atypical Lignification in Eastern Leatherwood (*Dirca palustris*)." *New Phytologist* 226, no. 3: 704–713.

Mottiar, Y., S. D. Karlen, R. E. Goacher, J. Ralph, and S. D. Mansfield. 2023. "Metabolic Engineering of *p*-Hydroxybenzoate in Poplar Lignin." *Plant Biotechnology Journal* 21, no. 1: 176–188.

Mottiar, Y., and S. D. Mansfield. 2022. "Lignin *p*-Hydroxybenzoylation Is Negatively Correlated With Syringyl Units in Poplar." *Frontiers in Plant Science* 13: 938083.

Mottiar, Y., R. Vanholme, W. Boerjan, J. Ralph, and S. D. Mansfield. 2016. "Designer Lignins: Harnessing the Plasticity of Lignification." *Current Opinion in Biotechnology* 37: 190–200.

Muro-Villanueva, F., X. Mao, and C. Chapple. 2019. "Linking Phenylpropanoid Metabolism, Lignin Deposition, and Plant Growth Inhibition." *Current Opinion in Biotechnology* 56: 202–208.

Musha, Y., and D. A. I. Goring. 1975. "Distribution of Syringyl and Guaiacyl Moieties in Hardwoods as Indicated by Ultraviolet Microscopy." *Wood Science and Technology* 9, no. 1: 45–58.

Mustafa, N. R., and R. Verpoorte. 2005. "Chorismate Derived C6C1 Compounds in Plants." *Planta* 222, no. 1: 1–5.

Nugroho, L. H., M. C. Verberne, and R. Verpoorte. 2002. "Activities of Enzymes Involved in the Phenylpropanoid Pathway in Constitutively Salicylic Acid-Producing Tobacco Plants." *Plant Physiology and Biochemistry* 40, no. 9: 755–760.

Pinard, D., and E. Mizrachi. 2018. "Unsung and Understudied: Plastids Involved in Secondary Growth." *Current Opinion in Plant Biology* 42: 30–36.

Poulsen, C., and R. Verpoorte. 1991. "Roles of Chorismate Mutase, Isochorismate Synthase and Anthranilate Synthase in Plants." *Phytochemistry* 30, no. 2: 377–386.

Qian, Y., J. H. Lynch, L. Guo, D. Rhodes, J. A. Morgan, and N. Dudareva. 2019. "Completion of the Cytosolic Post-Chorismate Phenylalanine Biosynthetic Pathway in Plants." *Nature Communications* 10, no. 1: 15.

Rai, V. K. 2002. "Role of Amino Acids in Plant Responses to Stress." *Biologia Plantarum* 45, no. 4: 481–487.

Robinson, A. R., and S. D. Mansfield. 2009. "Rapid Analysis of Poplar Lignin Monomer Composition by a Streamlined Thioacidolysis Procedure and Near-Infrared Reflectance-Based Prediction Modeling." *Plant Journal* 58, no. 4: 706–714.

Romero, R. M., M. F. Roberts, and J. D. Phillipson. 1995. "Chorismate Mutase in Microorganisms and Plants." *Phytochemistry* 40, no. 4: 1015–1025.

Sperry, J. S. 2003. "Evolution of Water Transport and Xylem Structure." *International Journal of Plant Sciences* 164, no. S3: S115–S127.

Stothard, P. 2000. "The Sequence Manipulation Suite: JavaScript Programs for Analyzing and Formatting Protein and DNA Sequences." *BioTechniques* 28, no. 6: 1102–1104.

Sundell, D., C. Mannapperuma, S. Netotea, et al. 2015. "The Plant Genome Integrative Explorer Resource: PlantGenIE.org." *New Phytologist* 208, no. 4: 1149–1156.

Sundell, D., N. R. Street, M. Kumar, et al. 2017. "AspWood: High-Spatial-Resolution Transcriptome Profiles Reveal Uncharacterized Modularity of Wood Formation in *Populus tremula*." *Plant Cell* 29, no. 7: 1585–1604.

Tohge, T., M. Watanabe, R. Hoefgen, and A. R. Fernie. 2013. "Shikimate and Phenylalanine Biosynthesis in the Green Lineage." *Frontiers in Plant Science* 4: 62.

Tsai, C.-J., S. A. Harding, T. J. Tschaplinski, R. L. Lindroth, and Y. Yuan. 2006. "Genome-Wide Analysis of the Structural Genes Regulating Defense Phenylpropanoid Metabolism in *Populus*." *New Phytologist* 172, no. 1: 47–62.

Tschaplinski, T. J., R. F. Standaert, N. L. Engle, et al. 2012. "Down-Regulation of the Caffeic Acid *O*-Methyltransferase Gene in Switchgrass Reveals a Novel Monolignol Analog." *Biotechnology for Biofuels* 5, no. 1: 71.

Tzin, V., and G. Galili. 2010. "New Insights Into the Shikimate and Aromatic Amino Acids Biosynthesis Pathways in Plants." *Molecular Plant* 3, no. 6: 956–972.

Tzin, V., S. Malitsky, A. Aharoni, and G. Galili. 2009. "Expression of a Bacterial Bi-Functional Chorismate Mutase/Prephenate Dehydratase Modulates Primary and Secondary Metabolism Associated With Aromatic Amino Acids in *Arabidopsis*." *Plant Journal* 60, no. 1: 156–167.

Unda, F., Y. Mottiar, E. L. Mahon, et al. 2022. "A New Approach to Zip-Lignin: 3, 4-Dihydroxybenzoate Is Compatible With Lignification." *New Phytologist* 235, no. 1: 234–246.

Vicente, M. R.-S., and J. Plasencia. 2011. "Salicylic Acid Beyond Defence: Its Role in Plant Growth and Development." *Journal of Experimental Botany* 62, no. 10: 3321–3338.

Waese, J., J. Fan, A. Pasha, et al. 2017. "ePlant: Visualizing and Exploring Multiple Levels of Data for Hypothesis Generation in Plant Biology." *Plant Cell* 29, no. 8: 1806–1821.

Wang, J. P., M. L. Matthews, P. P. Naik, et al. 2019. "Flux Modeling for Monolignol Biosynthesis." *Current Opinion in Biotechnology* 56: 187–192.

Westfall, C. S., A. Xu, and J. M. Jez. 2014. "Structural Evolution of Differential Amino Acid Effector Regulation in Plant Chorismate Mutases." *Journal of Biological Chemistry* 289, no. 41: 28619–28628.

Wise, A. A., Z. Liu, and A. N. Binns. 2006. "Three Methods for the Introduction of Foreign DNA Into *Agrobacterium*." In *Agrobacterium Protocols*, edited by K. Wang, vol. 1, Second ed., 43–54. Totowa, NJ, U.S.A: Humana Press.Volume 343 of *Methods in Molecular Biology*.

Woodin, T. S., L. Nishioka, and A. Hsu. 1978. "Comparison of Chorismate Mutase Isozyme Patterns in Selected Plants." *Plant Physiology* 61, no. 6: 949–952.

Xue, L.-J., W. Guo, Y. Yuan, et al. 2013. "Constitutively Elevated Salicylic Acid Levels Alter Photosynthesis and Oxidative State but Not Growth in Transgenic *Populus*." *Plant Cell* 25, no. 7: 2714–2730.

Zhong, R., and Z.-H. Ye. 2009. "Transcriptional Regulation of Lignin Biosynthesis." *Plant Signaling & Behavior* 4, no. 11: 1028–1034.

Zhong, S., Z. Chen, J. Han, H. Zhao, J. Liu, and Y. Yu. 2020. "Suppression of Chorismate Synthase, Which Is Localized in Chloroplasts and Peroxisomes, Results in Abnormal Flower Development and Anthocyanin Reduction in Petunia." *Scientific Reports* 10: 10846.

Supporting Information

Additional supporting information can be found online in the Supporting Information section.